

PAPER • OPEN ACCESS

Imaging slow brain activity during neocortical and hippocampal epileptiform events with electrical impedance tomography

To cite this article: Sana Hannan *et al* 2021 *Physiol. Meas.* **42** 014001

View the [article online](#) for updates and enhancements.

You may also like

- [Risk of seizures induced by intracranial research stimulation: analysis of 770 stimulation sessions](#)
Hannah E Goldstein, Elliot H Smith, Robert E Gross *et al.*
- [Non-invasive wearable seizure detection using long-short-term memory networks with transfer learning](#)
Mona Nasser, Tal Pal Attia, Boney Joseph *et al.*
- [Seizure forecasting using machine learning models trained by seizure diaries](#)
Ezequiel Gleichgerrcht, Mircea Dumitru, David A Hartmann *et al.*

The Breath Biopsy® Guide
Fourth edition

FREE

DOWNLOAD THE FREE E-BOOK

BREATH BIOPSY

OWLSTONE MEDICAL



PAPER

Imaging slow brain activity during neocortical and hippocampal epileptiform events with electrical impedance tomography

OPEN ACCESS

RECEIVED

31 October 2020

REVISED

21 December 2020

ACCEPTED FOR PUBLICATION






23 December 2020

PUBLISHED

4 February 2021

Original content from this work may be used under the terms of the [Creative Commons Attribution 4.0 licence](#).

Any further distribution of this work must maintain attribution to the author(s) and the title of the work, journal citation and DOI.

Sana Hannan^{1,*} , Kirill Aristovich¹ , Mayo Faulkner² , James Avery³ , Matthew C Walker⁴ and David S Holder¹ ¹ Department of Medical Physics and Biomedical Engineering, University College London, United Kingdom² Wolfson Institute for Biomedical Research, University College London, United Kingdom³ Department of Surgery and Cancer, Imperial College London, United Kingdom⁴ UCL Queen Square Institute of Neurology, University College London, United Kingdom

* Author to whom any correspondence should be addressed.

E-mail: sana.hannan@ucl.ac.uk**Keywords:** seizure, epilepsy, electrical impedance tomography, neocortex, hippocampus, slow activity**Abstract**

Objective. Electrical impedance tomography (EIT) is an imaging technique that produces tomographic images of internal impedance changes within an object using surface electrodes. It can be used to image the slow increase in cerebral tissue impedance that occurs over seconds during epileptic seizures, which is attributed to cell swelling due to disturbances in ion homeostasis following hypersynchronous neuronal firing and its associated metabolic demands. In this study, we characterised and imaged this slow impedance response during neocortical and hippocampal epileptiform events in the rat brain and evaluated its relationship to the underlying neural activity. **Approach.** Neocortical or hippocampal seizures, comprising repeatable series of high-amplitude ictal spikes, were induced by electrically stimulating the sensorimotor cortex or perforant path of rats anaesthetised with fentanyl-isoflurane. Transfer impedances were measured during ≥ 30 consecutive seizures, by applying a sinusoidal current through independent electrode pairs on an epicortical array, and combined to generate an EIT image of slow activity. **Main results.** The slow impedance responses were consistently time-matched to the end of seizures and EIT images of this activity were reconstructed reproducibly in all animals ($p < 0.03125$, $N = 5$). These displayed foci of activity that were spatially confined to the facial somatosensory cortex and dentate gyrus for neocortical and hippocampal seizures, respectively, and encompassed a larger volume as the seizure progressed. Centre-of-mass analysis of reconstructions revealed that this activity corresponded to the true location of the epileptogenic zone, as determined by EEG recordings and fast neural EIT measurements which were obtained simultaneously. **Significance.** These findings suggest that the slow impedance response presents a reliable marker of hypersynchronous neuronal activity during epileptic seizures and can thus be utilised for investigating the mechanisms of epileptogenesis *in vivo* and for aiding localisation of the epileptogenic zone during presurgical evaluation of patients with refractory epilepsies.

1. Introduction

Approximately 30% of people with epilepsy are refractory to the available anticonvulsant medication and may benefit from surgical resection of epileptogenic tissue for seizure control (Nair 2016). Over half of the patients who undergo resective surgery experience postoperative seizure relapse during the 10 year period after surgery which may be attributed to inaccurate presurgical localisation of the epileptogenic zone (Spencer *et al* 2005, de Tisi *et al* 2011). Electrical impedance tomography (EIT) is a medical imaging modality that holds potential for improving the accuracy with which the epileptogenic zone is localised and, consequently, the post-surgical outcome in these patients (Fabrizi *et al* 2006). EIT is able to image neural activity during epileptiform discharges

as deep as the hippocampus with a spatiotemporal resolution of 2 ms and $\sim 300\ \mu\text{m}$ from the rat cortical surface (Hannan *et al* 2020a). However, this method requires averaging of repetitive neural events over long recording periods to obtain an adequate signal-to-noise ratio (SNR) for imaging (Aristovich *et al* 2018, Hannan *et al* 2020a). An alternative approach is to use EIT to image the slower impedance signal that occurs secondarily to neural activity on a timescale of seconds during seizures. Due to the greater magnitude of this signal, and therefore the lack of needing to average, it could potentially be used to image epileptic activity in real time which would increase the applicability of EIT for use in clinical settings and *in vivo* research. This study focused on characterising and imaging this slow impedance response during seizures.

1.1. Background

1.1.1. Physiological basis of impedance changes during epileptiform activity

There are two main impedance changes which occur during epileptic seizures that may be imaged with EIT: the 'fast neural' and 'slow' responses. The fast neural impedance response occurs on a timescale of milliseconds and is due to the opening of voltage- and ligand-gated ion channels in the cell membrane of active neurons (Klvington and Galambos 1967, Oh *et al* 2011). This allows current to pass into the intracellular space, leading to a transient impedance decrease in the neural tissue (Aristovich *et al* 2016). The slow increase in cerebral tissue impedance that occurs over seconds during seizures has been reported during chemically and electrically induced seizures across several species (Van Harreveld and Schadé 1962, Elazar *et al* 1966, Olsson *et al* 2006). This impedance increase is attributed to cell swelling which arises as a result of the high metabolic demands of intense neuronal activity during ictal events and causes the active cerebral tissue to outrun its available energy supplies, giving rise to anoxic depolarisation (Andrew and MacVicar 1994, Dzhalala *et al* 2000, Dreier *et al* 2011). This state of uncontrolled neuronal depolarisation is induced by loss of regulation of the membrane sodium-potassium adenosine triphosphatase (Na^+/K^+ -ATPase) pump which is normally responsible for maintaining the cell resting membrane potential (Hansen 1985, Balestrino 1995, Hille 2001). The resulting disturbance of ion homeostasis thus generates an osmotic gradient, leading to the movement of water from the extracellular space into the intracellular compartment, causing cell swelling (Hansen 1985, Hille 2001, Ullah *et al* 2015). When applied to cerebral tissue at a carrier frequency $< 50\ \text{kHz}$, the majority of current is conducted through the extracellular fluid and does not cross the highly resistive neuronal membrane (Holder 2005, Seoane *et al* 2005). By reducing the volume of extracellular fluid, cell swelling therefore causes an increase in the measured cerebral tissue impedance. Although the predominant mechanism of the slow impedance increase during seizures is expected to be cell swelling due to the increased metabolic demands of epileptiform activity, there may be a minor influence of increased local cerebral blood flow and the associated small intracerebral temperature increase during seizures on the measured tissue impedance. Increased cerebral blood flow will cause an opposing impedance decrease but this is likely to be much smaller than the increase due to cell swelling, since capillaries count for only $\sim 2\%$ of the cerebral volume, and may not be in phase with the electrographic features of seizures or the measured tissue impedance response (Weiss 1988, Bahar *et al* 2006, Shariff *et al* 2006, Schwartz 2007). Focal seizures may also result in a relatively small localised increase in intracerebral temperature of $0.3\ ^\circ\text{C}$, but this is likely to have a negligible effect on the measured impedance (Yang *et al* 2002, Holder 2005).

1.1.2. EIT of epileptiform activity

EIT produces tomographic images of internal electrical impedance changes within an object. These images are reconstructed from multiple transfer impedance measurements made with non-penetrating electrodes on the surface of the object (Holder 2005). Each transfer impedance measurement is obtained by injecting current through a single electrode pair and recording the resulting boundary voltages from all other available electrodes. EIT can be used to image both the fast neural and slow impedance responses during epileptiform activity.

1.1.2.1. Imaging the fast neural impedance change

Previous fast neural EIT studies have shown that EIT can image neural activity during ictal and interictal epileptiform discharges, induced by chemical and electrical models of epilepsy, as deep as the hippocampus using non-penetrating electrodes implanted on the cortical surface of the anaesthetised rat (Vongerichten *et al* 2016, Hannan *et al* 2018a, 2020a). In these studies, an epicortical array containing up to 57 electrodes was implanted on the rat cortex and impedance measurements were recorded by sequentially injecting current through electrode pairs. To image ictal spikes during neocortical or hippocampal seizures, an independent impedance measurement was obtained during each of 30 reproducible seizures and the impedance changes associated with repeatable spikes were averaged within seizures. This averaging is a requirement to improve SNR by noise reduction due to the low magnitude of the fast neural impedance signal during ictal spikes ($\leq 0.3\%$) (Hannan *et al* 2018a, 2020a). To extract impedance signals, a bandpass filter with a $\pm 500\ \text{Hz}$ bandwidth around the carrier frequency of injected current was used which gave a temporal resolution of 2 ms. The resulting

images showed neural impedance changes every 2 ms over a 40 ms epoch during a single averaged ictal spike. Due to the need for averaging, however, fast neural EIT currently requires seizures with highly reproducible ictal spikes and does not enable imaging over the course of the entire seizure.

1.1.2.2. *Imaging the slow impedance change*

Imaging the slow impedance response over the course of a seizure may present a method for overcoming the limitations of fast neural EIT. At any given carrier frequency of injected current, the amplitude of the slow impedance response is up to ten times larger than that of the fast neural impedance change during averaged ictal discharges (Rao 2000, Vongerichten *et al* 2016, Hannan *et al* 2018b). As a result, slow impedance responses can be imaged over epochs that encompass entire seizures (≥ 90 s) without requiring averaging. Moreover, this approach may ultimately enable single-shot imaging of individual seizures using parallel multifrequency EIT, in which current is injected simultaneously through multiple electrode pairs at different carrier frequencies (Dowrick *et al* 2015). Imaging fast neural activity is not currently possible with parallel EIT because all chosen frequencies of injected current would need to be separated by ≥ 500 Hz, the required bandwidth for getting a 2 ms temporal resolution. Further, the magnitude and SNR of the fast neural impedance response is dramatically reduced at carrier frequencies above 2 kHz which severely limits the number of parallel current injections that can be used for producing fast neural EIT images (Hannan *et al* 2018b). In contrast, the slow impedance change can be imaged with a 1 s temporal resolution, meaning that a bandwidth as low as 1 Hz around the carrier frequency can be used to extract the signal. Because the magnitude and SNR of the slow impedance change is not significantly different across frequencies in the 1–10 kHz range, hundreds of simultaneous current injections could theoretically be utilised for reconstructing an EIT image of the slow activity during a single seizure with high spatial accuracy (Hannan *et al* 2018b, Hannan 2019). This method would be highly beneficial for any clinical or research application in which seizures occur infrequently or unpredictably. However, the slow impedance response is typically a secondary phenomenon that occurs as a by-product of the neural event itself. Therefore, prior to implementing EIT protocols aimed at imaging this slow activity, it is important to characterise its spatiotemporal features and validate that it is indeed representative of the fast neural activity during the epileptiform event and thus a reliable biomarker of the ictal onset zone. This was addressed in the present study.

1.1.3. *In vivo models of epileptiform activity*

For evaluating the technical accuracy of EIT for imaging impedance responses during seizures, the induced epileptiform events need to have a consistent well-defined focal origin and be highly reproducible in their electrographic characteristics. For these reasons, the neocortical and hippocampal epileptic afterdischarge models were selected. In these models, electrical stimulation of the sensorimotor cortex or perforant path results in the immediate induction of epileptiform events lasting ≥ 10 s on demand, which will henceforth be referred to as ‘seizures’, with foci localised to the facial somatosensory cortex or dentate gyrus, respectively (Hannan *et al* 2020b). As such, use of these models enabled assessment of slow and fast impedance changes at two different depths of activity. In addition, the induced seizures comprised trains of ictal spikes which exhibited a high degree of repeatability and thus were suitable for averaging; this was required to image fast neural impedance changes for direct comparison to the concurrently imaged slow activity during seizures.

1.2. Purpose

This study was aimed at determining whether EIT can be used to image slow impedance responses during seizures, from the surface of the rat cortex, and evaluating the potential of the imaged slow activity to act as a valid indicator of the epileptogenic zone. Specific sub-questions to address were as follows.

- (i) What are the spatiotemporal features of the slow activity imaged during seizures and how do these compare to the simultaneously obtained EEG recordings and fast neural EIT images?
- (ii) Can this method be used to image deeper epileptiform activity in the hippocampus as well as superficial neocortical activity?

1.3. Experimental design

Impedance measurements during neocortical and hippocampal epileptic seizures were previously recorded from the surface of the cerebral cortex of anaesthetised rats using a planar epicortical electrode array (Hannan *et al* 2018a, 2020a). Since the induced neocortical and hippocampal seizures were highly reproducible and remained electrographically stable over time, it was possible to obtain an impedance recording during each seizure using an independent pair of EIT current-injecting electrodes. A single imaging protocol comprised at least 30 sequential impedance measurements obtained in 30 consecutive neocortical or hippocampal seizures.

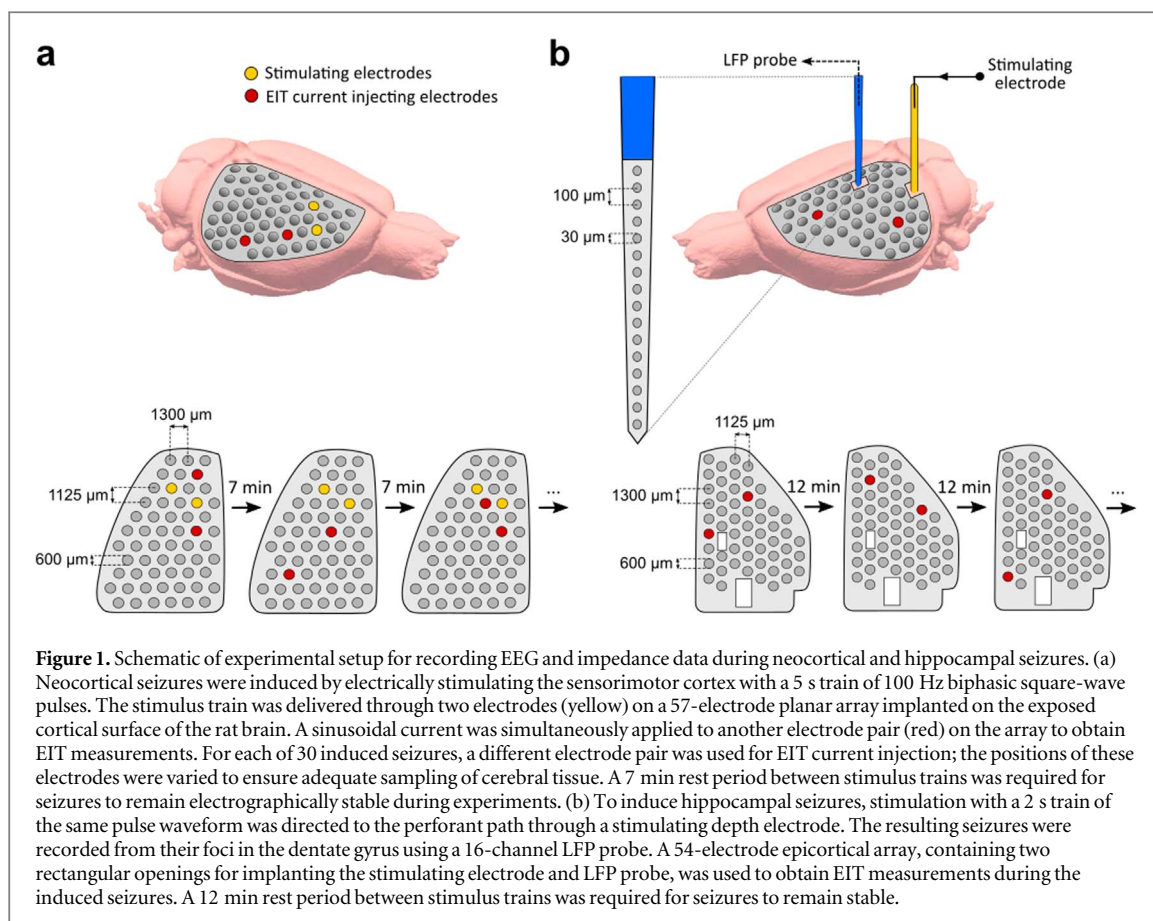
The EIT recordings contained both the slow and fast neural impedance signals which can be extracted from the raw data using a bandpass filter with differing bandwidths around the carrier frequency, namely, ± 1 Hz and ± 500 Hz, respectively. The fast neural EIT measurements obtained from these datasets have previously been imaged (Hannan *et al* 2018a, 2020a) and are reused here only for direct comparison to the concomitant slow impedance changes during seizures. The imaged slow activity was assessed for reproducibility across animals and compared to fast neural reconstructions using centre-of-mass analysis. Further analysis was performed to determine whether the slow impedance changes were correlated to fast neural impedance changes and EEG recordings obtained during neocortical and hippocampal seizures. As such, we were able to establish whether the slow impedance response can be used as a reliable and more robust biomarker of the hypersynchronous neural activity underlying epileptiform events that can overcome the limitations of fast neural EIT.

2. Materials and methods

2.1. Data collection

This study utilised two datasets that were collected previously. For retrospective analysis of slow impedance data from neocortical seizures, we used data from experiments performed in five female Sprague-Dawley rats (300–450 g) by Hannan *et al* (2018a). For analysis of slow impedance data from hippocampal seizures, we used data generated in five female Sprague-Dawley rats (405–460 g) by Hannan *et al* (2020a). Please refer to these previous studies for a detailed description of methods employed in the neocortical and hippocampal imaging experiments (Hannan *et al* 2018a, 2020a). A brief overview of the experimental procedures, provided for reader convenience, is as follows.

Rats were anaesthetised with fentanyl-isoflurane and a planar epicortical electrode array was implanted on the cortical surface of one hemisphere. For neocortical imaging experiments, a 57-electrode epicortical array was used and seizures were elicited by electrically stimulating the sensorimotor cortex. For hippocampal imaging experiments, the epicortical array contained 54 electrodes and two openings for implanting: (a) a stimulating depth electrode targeting the perforant path to induce focal hippocampal seizures, and (b) a 16-channel local field potential (LFP) probe for recording from the dentate gyrus to confirm the presence of ictal activity. Seizures were induced by stimulating the sensorimotor cortex or perforant path, respectively, with 100 Hz trains of biphasic square-wave pulses in accordance with the adapted neocortical and hippocampal epileptic afterdischarge models (Hannan *et al* 2020b). Minimum inter-train intervals of 7 and 12 min, respectively, ensured that baseline activity was restored after seizure induction and that seizure patterns remained electrographically stable during experiments. If any motor manifestations of seizures were observed, rats were paralysed prior to commencing EIT recordings with pancuronium bromide (1 mg kg^{-1}), administered intravenously. As such, the EEG and EIT recordings remained uncontaminated by movement artefacts. During each seizure, ECoG/LFP and EIT data were obtained simultaneously. For the latter, a sinusoidal current was applied to a pair of epicortical electrodes and voltage measurements were obtained for the resulting current pattern from all other electrodes on the epicortical array. The parameters for EIT measurements were chosen for the initial purpose of imaging fast neural impedance changes, which are approximately ten times smaller in magnitude than the slow impedance responses that were obtained simultaneously and extracted from the same datasets (Hannan *et al* 2018b). For neocortical seizures, the EIT current was applied at an amplitude of $50 \mu\text{A}$ and a carrier frequency of 1.725 kHz, in accordance with a previous *in vivo* EIT study in which these parameters were used to successfully image fast neural impedance changes during physiological activity in the rat neocortex (Aristovich *et al* 2016). Because the sensitivity of EIT to impedance changes is known to decrease with distance from the electrodes, the SNR of hippocampal impedance changes as measured from the cortical surface is expected to be considerably lower than that of cortical impedance changes (Faulkner *et al* 2018b). Therefore, it was important to use optimal recording parameters to maximise the chances of imaging fast neural ictal activity in the hippocampus using epicortical electrodes. For this reason, we used EIT current with an amplitude of $100 \mu\text{A}$ in the hippocampal imaging experiments; this is the highest current level that can be applied continuously to the rat cerebral cortex without affecting the amplitude or latency of neural activity or causing structural damage to the cortical tissue (Oh *et al* 2011, Hannan *et al* 2019). Additionally, current was applied at 1.355 kHz, the optimal carrier frequency for imaging impedance changes during epileptiform events (Hannan *et al* 2018b). Use of these parameters resulted in successful imaging of both the fast and slow impedance changes during neocortical and hippocampal ictal activity, thereby enabling their direct comparison. A full EIT protocol consisted of at least 30 sequential impedance measurements, each obtained during a single seizure with an independent electrode pair for current injection (figure 1). Control recordings were used to confirm that the measured impedance responses were not artefactual and were indeed caused by the evoked seizures. These included baseline EEG and impedance recordings, obtained prior to stimulus application, and full post-mortem EIT protocols. All animal handling and experimental investigations were ethically approved by the UK Home



Office and performed in accordance with its regulations, as outlined in the Animals (Scientific Procedures) Act 1986.

2.2. Analysis of EEG and impedance data

All recordings were taken during a time window that included the seizure as well as ≥ 10 s pre-stimulation and ≥ 30 s post-ictal baseline periods. The raw voltage measurements contained the EEG and fast and slow impedance data; these were extracted with different filters. The ECoG and LFP signals were extracted by applying a first order, high-pass filter at 1 Hz, a Butterworth filter at 1 kHz (low-pass, fifth order), and a notch filter at 50 Hz (IIR, second order). The slow impedance signals were extracted by applying a ± 1 Hz bandpass Butterworth filter (third order) either side of the carrier frequency, 1.725 kHz for neocortical seizures and 1.355 kHz for hippocampal seizures, which yielded a 1 s temporal resolution. The fast impedance signals were obtained previously by applying a ± 500 Hz bandpass Butterworth filter (fifth order) around the carrier frequency in recordings from neocortical (Hannan *et al* 2018a) and hippocampal seizures (Hannan *et al* 2020a); this fast neural data is used here only for direct comparison to concomitant slow impedance changes during seizures. The slow impedance signals were demodulated using the Hilbert transform and processed for image reconstruction. Please refer to previous studies for a detailed description of the analysis of the fast neural EIT signal during neocortical and hippocampal ictal discharges (Hannan *et al* 2018a, 2020a).

Seizures were defined as the sudden appearance of abnormal electrographic activity in the ECoG or LFP traces for neocortical and hippocampal seizures, respectively, which had a minimum duration of 10 s and comprised a series of high-amplitude (> 2 times baseline activity) rhythmic ictal discharges. The seizure start time was marked by the first of these ictal discharges and seizure duration was defined as the time period between the first and last ictal discharge. ECoG and LFP recordings were used to confirm that the foci and electrographic patterns of seizures remained stable over the course of the EIT protocol so that impedance data from multiple seizures, obtained using different spatial configurations of current-injecting electrodes, could be combined to reconstruct an image of the slow impedance change during a typical neocortical or hippocampal ictal event.

The slow impedance change (dZ) that occurred during each seizure could be visualised in the demodulated impedance traces. The impedance trace recorded from each channel was normalised to the baseline dZ , defined as the mean amplitude during the 5 s period immediately preceding delivery of the electrical stimulus for seizure induction. Current-injecting and disconnected channels were identified and rejected from further analysis. dZ

measurements from all other epicortical electrode channels were collated across the 30 seizures by aligning the traces with respect to the start of the seizure and truncating the recordings according to the length of the seizure with the shortest duration recorded during a given EIT protocol. These processed dZ measurements were then used to generate an EIT image of slow activity during a neocortical or hippocampal seizure in each animal.

2.3. Tomographic reconstruction of slow impedance changes during seizures

EIT images of slow activity over the course of the entire seizure were reconstructed using ≤ 1650 processed voltages for neocortical seizures and ≤ 1560 processed voltages for hippocampal seizures. The total numbers of these voltage traces were determined by the number of epicortical channels available for recording during each impedance measurement. For every current injection protocol, the forward solution and the resulting Jacobian matrix were calculated on a finite element method (FEM) mesh of the rat brain, which contained 2.9 million tetrahedral elements, using the PEITS forward solver (Jehl *et al* 2015). Tissue conductivity values within the mesh were set to 0.3, 0.15 and 1.79 Sm^{-1} for the grey matter, white matter and cerebrospinal fluid, respectively (Ranck 1963, Baumann *et al* 1997, Latikka *et al* 2001, Horesh 2006). Imaging was performed using the time-difference EIT approach, based on the principle that most modelling errors cancel out when a reference baseline measurement is subtracted from the data measurement (Brown 2003). As such, the overall effects of the chosen conductivity values for the grey matter, white matter and cerebrospinal fluid in the rat brain mesh on the final reconstructed images are minimal (Brown 2003, Jehl *et al* 2016). The inverse problem was computed using an inversion of the Jacobian matrix. Images of slow activity were reconstructed at 1 s time steps for the entire seizure epoch on a $300 \mu\text{m}$ hexahedral mesh. Zeroth-order Tikhonov regularisation with noise-based correction was used for image reconstruction after selecting the regularisation parameter through generalised cross-validation (Tikhonov *et al* 1995, Aristovich *et al* 2014). The reconstructed conductivity values in each voxel were expressed as t-score ($\delta\sigma$) for visualisation. To calculate this, the conductivity change was divided by the computed standard deviation of the estimated conductivity change in a given element due to random Gaussian noise, in accordance with a previously described noise-based correction approach (Aristovich *et al* 2014).

2.4. Analysis of reconstructed images

To assess the reproducibility of the reconstructed slow activity during neocortical and hippocampal seizures, population statistics were undertaken in each group of five rats. Active voxels, defined as $\delta\sigma \geq 3$ ($p < 0.01$), were labelled in each reconstruction and the volume of active voxels that were common to all five animals ($p < 0.03125$) was identified by applying a binomial mask. The centre of mass of the slow activity was calculated at the peak time point in each image after applying the full width at half maximum (FWHM) filter, which thresholds the reconstruction at 50% of the maximal $\delta\sigma$. To delineate the brain regions that were activated during the induced neocortical and hippocampal seizures, qualitative evaluation of reconstructions was undertaken by visually inspecting the images with respect to an anatomical rat brain atlas (Paxinos and Watson 2013).

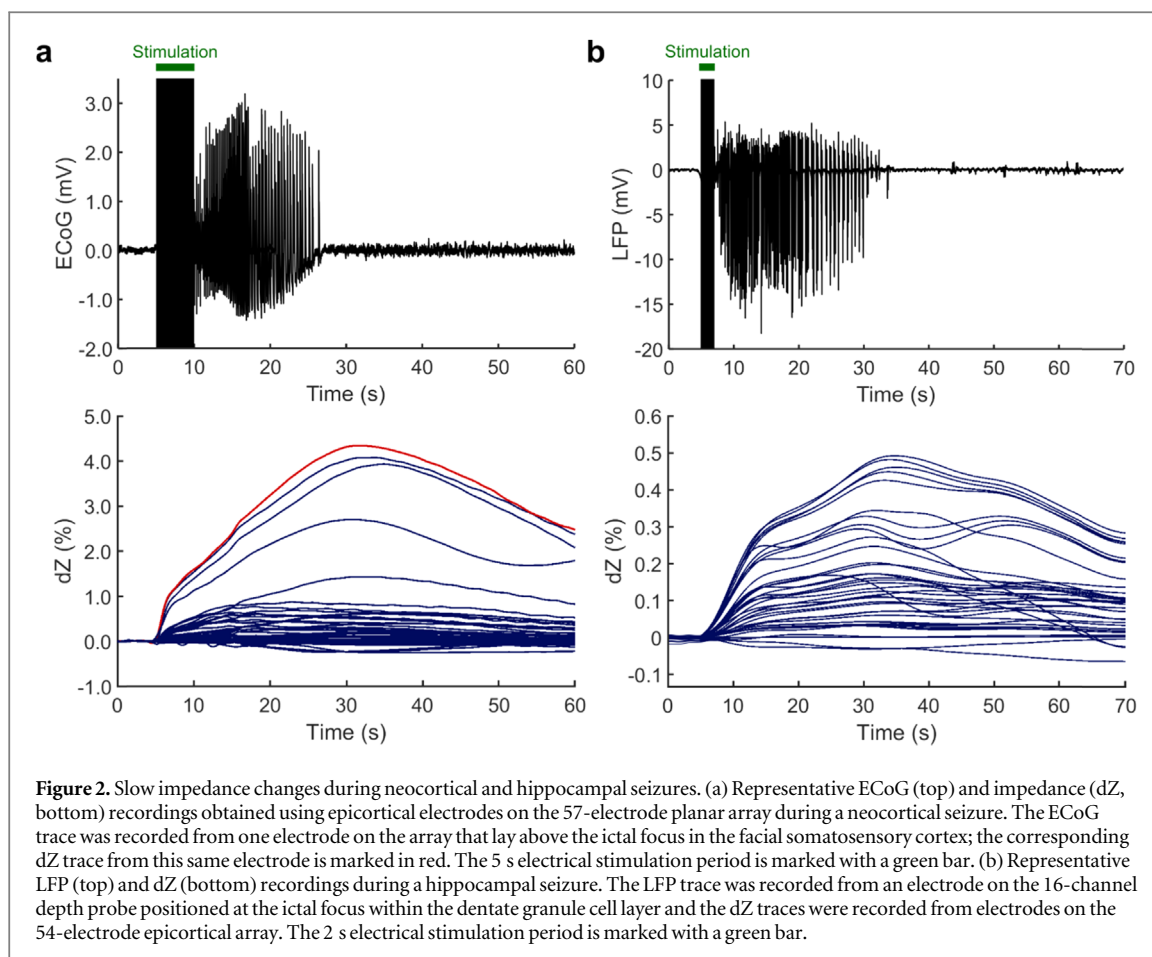
2.5. Comparison of slow impedance changes to EEG activity and fast neural impedance changes

The relationship between the maximal amplitude of the slow impedance change in the processed voltages and the maximal local EEG amplitude of the averaged ictal spike for a given seizure was evaluated using the Pearson's correlation coefficient. The same method was used to determine whether this maximal slow impedance amplitude and the time taken to reach it, measured from the beginning of the seizure, were correlated to the seizure duration. In addition, the Pearson's correlation coefficient was used to define the relationship between the maximal amplitudes of the slow and fast neural impedance changes for all induced seizures. A significance level of $\alpha = 0.01$ was used for all statistical analyses. For both neocortical and hippocampal seizures, the mean centre of mass of reconstructed slow and fast neural activity was calculated across animals. The mean centre of mass positions of the slow and fast neural reconstructions were directly compared and qualitatively evaluated by visualising them with respect to the Paxinos and Watson anatomical atlas (Paxinos and Watson 2013). All data are presented as mean \pm standard deviation.

3. Results

3.1. Characterising the slow impedance response to neocortical and hippocampal seizures

Neocortical seizures had a mean duration of 16.5 ± 5.3 s and were characterised by a series of repetitive high-amplitude cortical spike-and-wave discharges (SWDs) with a frequency of 2–5 Hz ($n = 168$ seizures, $N = 5$ rats). The slow impedance response during these seizures took the form of a steady increase in cortical tissue impedance over the course of the seizure which reached a maximal amplitude of $4.33\% \pm 0.89\%$ (figure 2(a)), several seconds after the last ictal discharge, at 21.1 ± 4.6 s relative to the beginning of the seizure. Following this



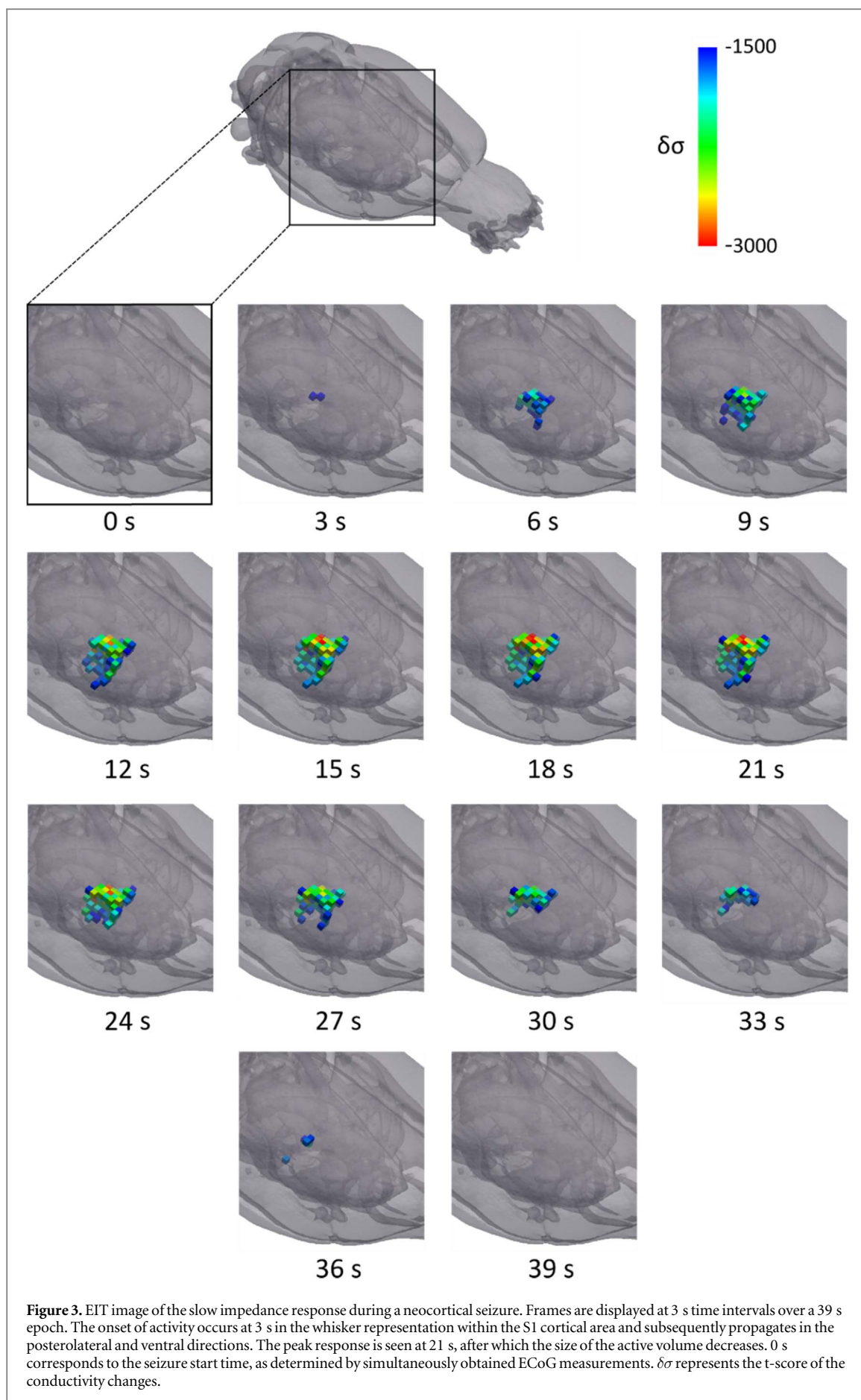
peak, the slow dZ proceeded to return to baseline until the end of the recording. Although it was not always possible to see a complete return to baseline by the end of the recording epoch, a distinct peak in the slow dZ was observed consistently for every seizure. In all induced seizures, the maximal slow impedance change and the highest-amplitude ictal discharges in the ECoG traces were both recorded from the same electrode on the epicortical array, which lay above the facial somatosensory cortex and corresponded to the ictal focus.

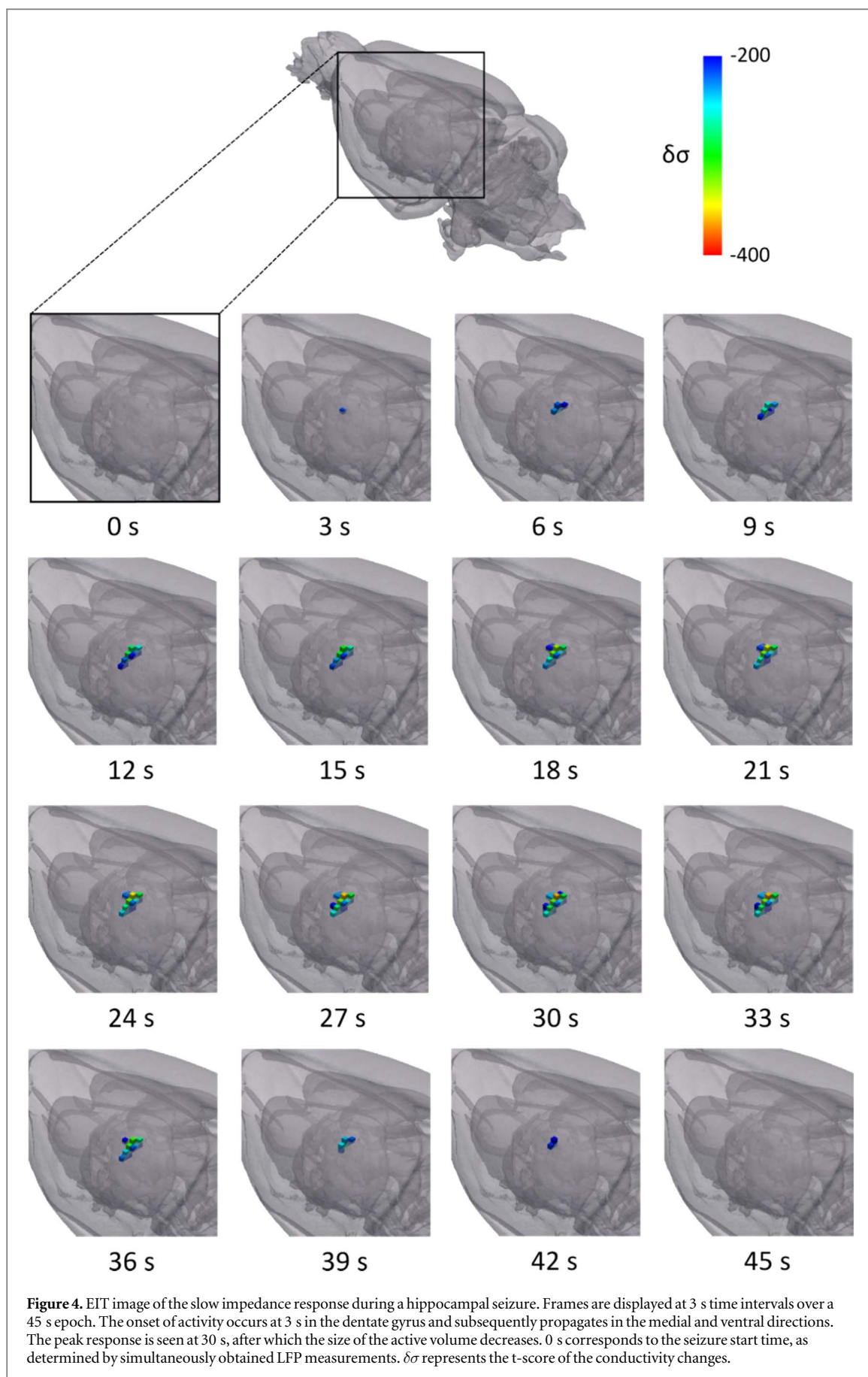
Hippocampal seizures had a mean duration of 28.3 ± 9.5 s and were characterised by a rhythmic pattern of high-amplitude granule cell population spikes, with a focus in the dentate granule cell layer of the hippocampus, at a frequency of 30–50 Hz ($n = 162$ seizures, $N = 5$ rats). As with the neocortical seizures, the dZ response to hippocampal seizures was marked by a slow increase in impedance that was in phase with LFP recordings of the seizure obtained from the dentate gyrus. The slow dZ reached a maximal amplitude of $0.52\% \pm 0.06\%$ (figure 2(b)) at 29.7 ± 9.2 s relative to the beginning of the seizure, which was followed by a decrease towards baseline.

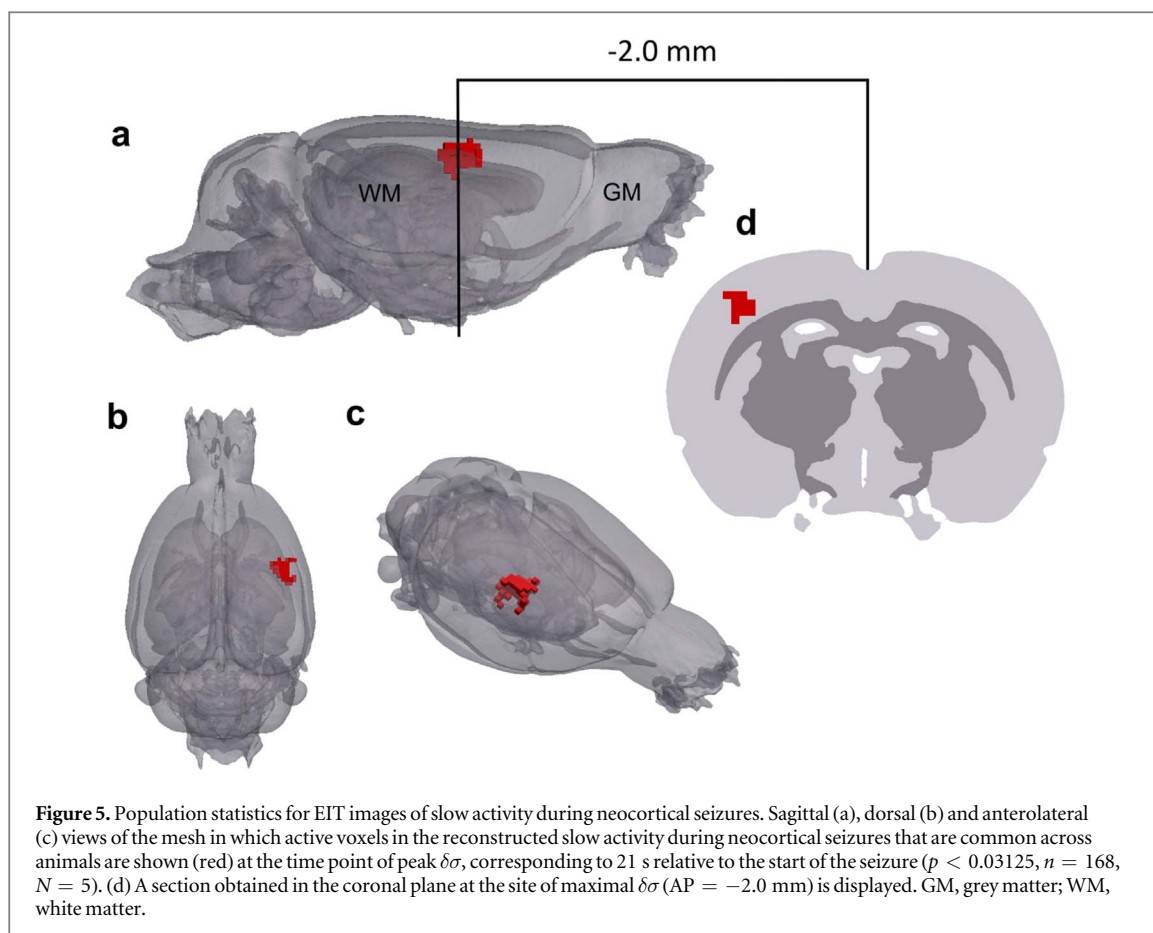
3.2. EIT images of slow activity during neocortical and hippocampal seizures

EIT images of the slow impedance response during neocortical and hippocampal seizures were reconstructed at 1 s time steps over a total period of 0 s to ≥ 60 s, where 0 s corresponded to the seizure start time. This time period encompassed the entire seizure in addition to a post-ictal baseline period. For neocortical seizures, the earliest significant slow activity was observed at 3 s within the barrel cortex area of the primary somatosensory cortex (S1) (figure 3; $n = 168$ seizures, $N = 5$ rats). This early activity was 3 mm posterior to the sensorimotor cortical region (M1/S1 HL) that was electrically stimulated to induce seizures and increased in volume between 3 and 21 s as the seizure progressed. During the seizure, the slow activity propagated posterolaterally and ventrally. After the peak response at 21 s, the volume of active voxels gradually decreased until 39 s, at which point no more significant activity was observed in the rest of the image.

For hippocampal seizures, the onset of slow activity occurred at 3 s within the dorsal region of the dentate gyrus and its structural centre in the anteroposterior axis (figure 4; $n = 162$ seizures, $N = 5$ rats). The active volume then increased over the course of the seizure, propagating in the medial and ventral directions and reaching a peak at 30 s. At this time point, the reconstructed activity encompassed most of the dentate gyrus and







extended to the medial region of the CA3 subfield of the hippocampus proper. Following the peak, the active volume progressively reduced in size until 45 s, from which point no further significant $\delta\sigma$ was seen.

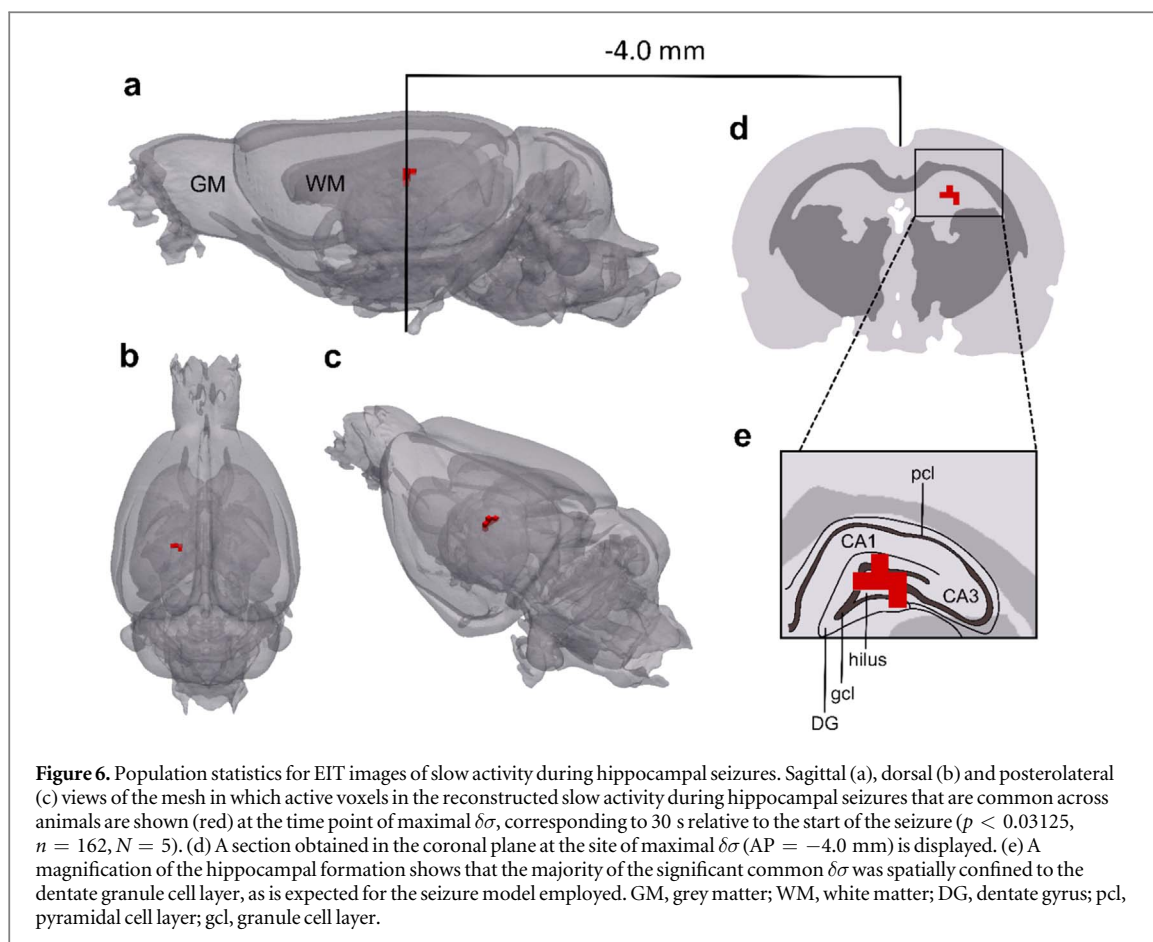
3.3. Reproducibility of EIT images of slow activity

After applying a binomial mask to determine image reproducibility, a spatially distinct volume of common active voxels during the reconstructed slow activity was observed across all rats in both neocortical (figure 5; $p < 0.03125$, $n = 168$ seizures, $N = 5$ rats) and hippocampal seizures (figure 6; $p < 0.03125$, $n = 162$ seizures, $N = 5$ rats). These common regions of slow activity matched the location of reconstructed $\delta\sigma$ within the facial representation of the S1 cortical area or dentate gyrus, respectively, for individual animals. Baseline and post-mortem control recordings confirmed that the reconstructions were not due to artefacts. These recordings, which were processed using the same methods as the induced ictal events, showed no significant activity in reconstructions (baseline: $n = 168$ recordings, $N = 5$ rats for neocortical imaging experiments; $n = 162$ recordings, $N = 5$ rats for hippocampal imaging experiments; post-mortem: $n = 60$ recordings, $N = 2$ rats each for neocortical and hippocampal imaging experiments).

3.4. Slow impedance changes are correlated to fast neural impedance changes and EEG activity during seizures

The Pearson's correlation coefficient was used to analyse the relationship between the slow impedance changes, the fast neural impedance changes and the ECoG or LFP recordings obtained during neocortical and hippocampal seizures. For neocortical seizures, the peak amplitude of the slow dZ was significantly correlated to the peak amplitude of the averaged ictal spike in the ECoG recordings (figure 7(a); $r = 0.74$, $p < 0.01$, $n = 168$ seizures, $N = 5$ rats) but not to the seizure duration (figure 7(b); $r = 0.06$, $p > 0.01$). The time taken for the slow dZ to reach its peak, measured from the beginning of the seizure, was correlated to the seizure duration (figure 7(c); $r = 0.95$, $p < 0.01$) and the peak amplitudes of the slow dZ during seizures and the fast neural dZ during averaged ictal SWDs were also significantly correlated (figure 7(d); $r = -0.79$, $p < 0.01$).

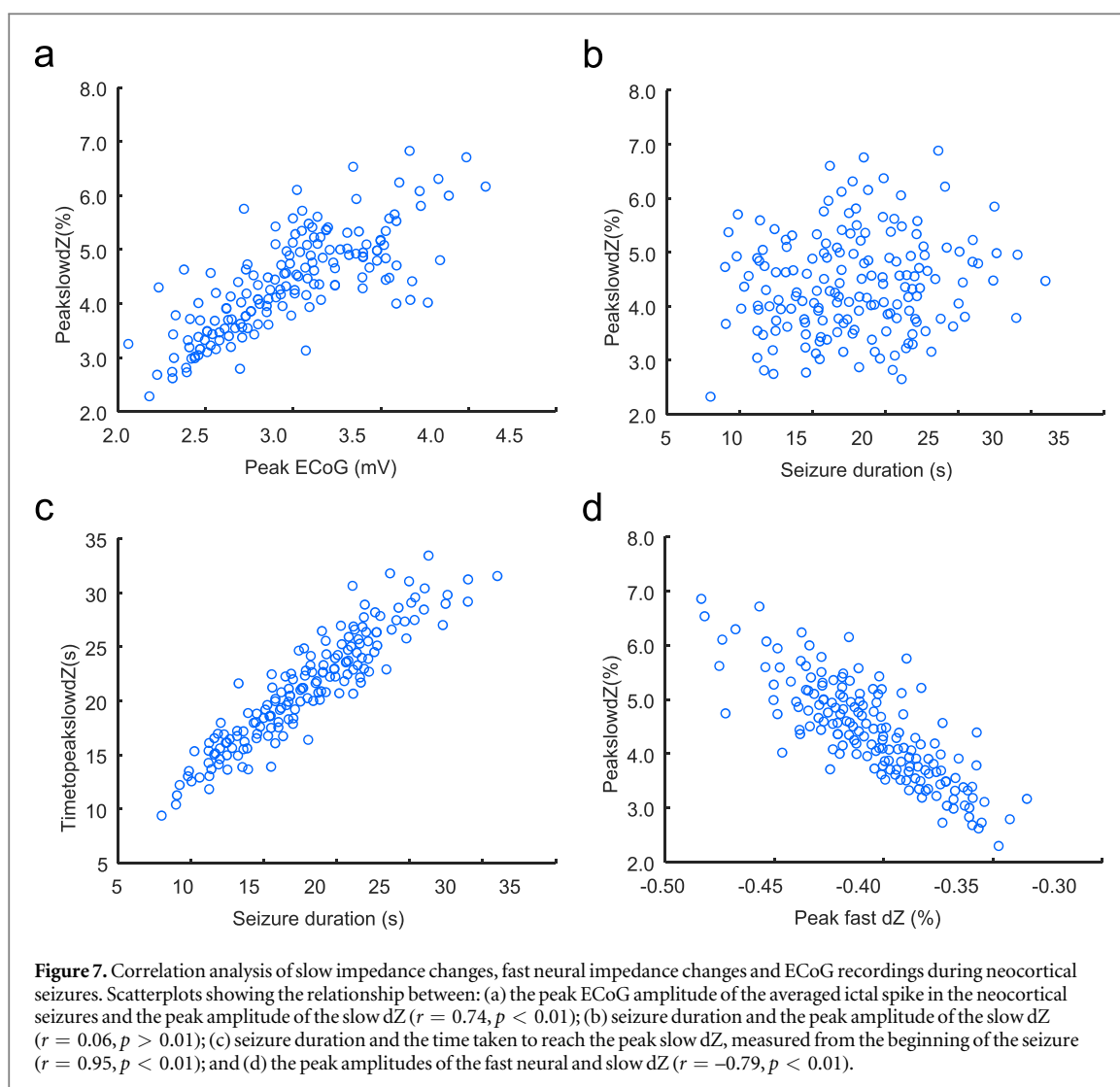
The correlation analysis for hippocampal seizures showed similar results. The peak amplitude of the slow dZ was also significantly correlated to both the peak amplitude of the averaged ictal granule cell population spikes in the LFP recordings (figure 8(a); $r = -0.71$, $p < 0.01$, $n = 162$ seizures, $N = 5$ rats) and the peak amplitude of the fast neural dZ during these averaged ictal spikes (figure 8(d); $r = -0.63$, $p < 0.01$). Again, the seizure duration



was not correlated to the peak amplitude of the slow dZ (figure 8(b); $r = 0.14$, $p > 0.01$) but was significantly correlated to the time taken to reach the peak slow dZ (figure 8(c); $r = 0.88$, $p < 0.01$).

For neocortical seizures, the mean centre of mass of the slow impedance change across rats at the peak $\delta\sigma$ lay within the facial somatosensory cortex and was positioned at: $AP = -2.1 \pm 0.1$ mm, $ML = 4.8 \pm 0.2$ mm, and $DV = 1.4 \pm 0.2$ mm measured from the cortical surface ($n = 168$ seizures, $N = 5$ rats). In contrast, the fast neural impedance change for averaged SWDs in the neocortical seizures exhibited a bimodal spatial profile of activation where two distinct regions of maximal $\delta\sigma$ were observed within the S1 cortical area (Hannan *et al* 2018a). The centre of mass positions for each of these active volumes, calculated at the peak $\delta\sigma$, were located at: (a) $AP = -2.0 \pm 0.2$ mm, $ML = 4.9 \pm 0.2$ mm, and $DV = 1.4 \pm 0.3$ mm; and (b) $AP = -4.1 \pm 0.2$ mm, $ML = 4.6 \pm 0.2$ mm, and $DV = 1.2 \pm 0.3$ mm. The centre of mass of the anterior-most volume of active voxels (a) for the fast neural dZ, which was observed at the earlier time point during the SWD and was larger in size than the more posterior volume of activity, matched the centre of mass of the slow activity in the S1 barrel cortex. Additionally, of all electrodes on the epicortical array, this centre of mass position was closest in proximity to the epicortical electrode from which the highest-amplitude ictal spikes were seen in ECoG traces during seizures, which was deemed to lie above the ictal focus.

The reconstructed centre of mass of the peak slow $\delta\sigma$ during hippocampal seizures was located in the medial section of the dentate granule cell layer. The mean centre of mass position across images was positioned at: $AP = -4.1 \pm 0.2$ mm, $ML = 2.6 \pm 0.2$ mm, and $DV = 3.0 \pm 0.3$ mm ($n = 162$ seizures, $N = 5$ rats). Its distance from the ictal focus, defined as the region of highest-amplitude ictal granule cell population spikes which was the targeted recording region for the 16-channel LFP probe ($AP = -4.0$, $ML = 2.5$, $DV = 2.8$ mm), was $100 \mu\text{m}$ in the anteroposterior and mediolateral axes and $200 \mu\text{m}$ in the dorsoventral axis. The centre of mass coordinates of the peak fast neural $\delta\sigma$, on the other hand, were: $AP = -4.1 \pm 0.2$ mm, $ML = 2.4 \pm 0.3$ mm, and $DV = 3.2 \pm 0.4$ mm (Hannan *et al* 2020a). As such, the localisation accuracy achieved in reconstructions of the slow dZ during hippocampal seizures ($\leq 200 \mu\text{m}$) was superior to that obtained in the fast neural dZ reconstructions ($\leq 400 \mu\text{m}$).

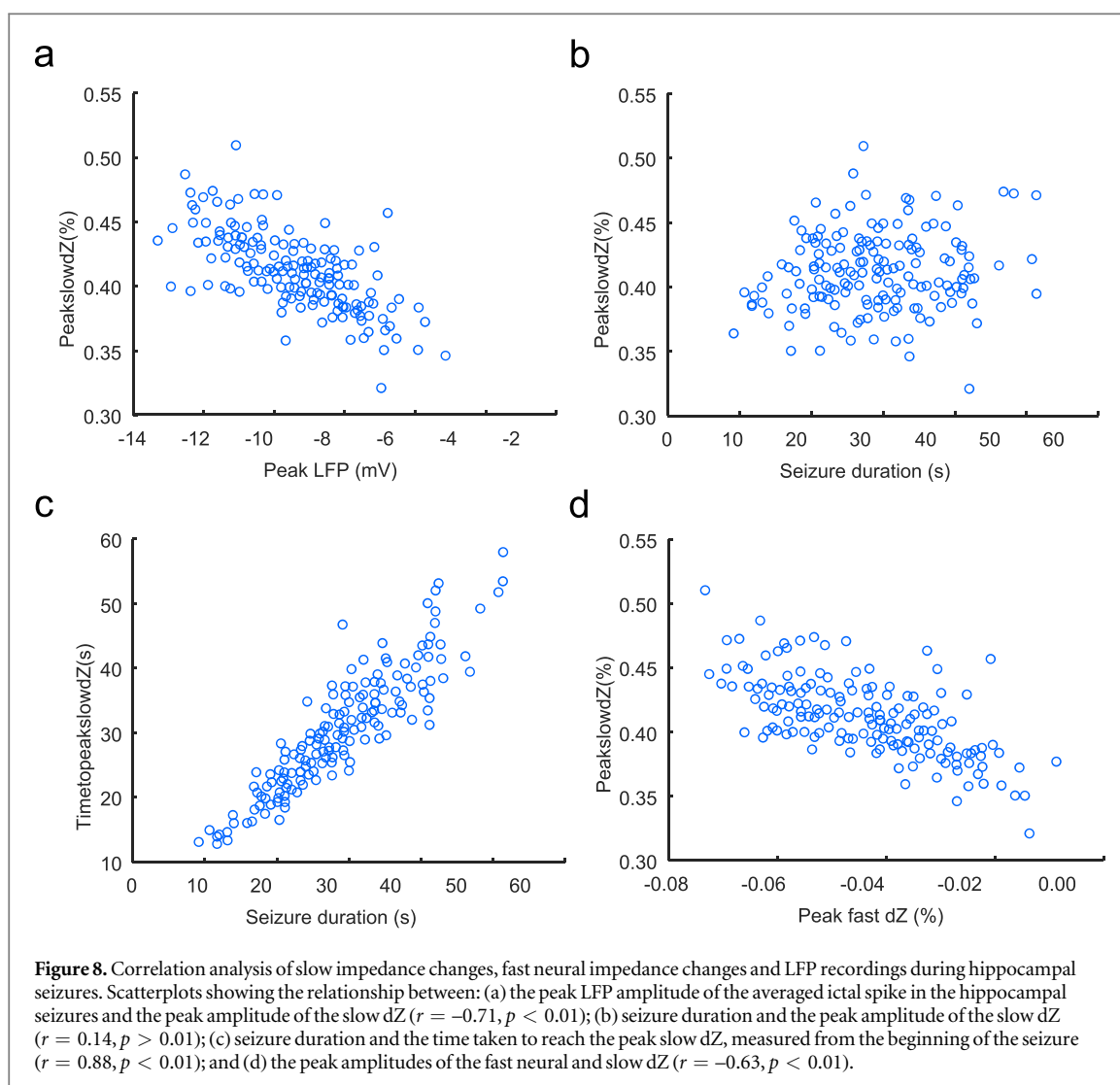


4. Discussion

In this study, we characterised and imaged the slow impedance response during neocortical and hippocampal seizures with EIT using non-penetrating electrodes implanted on the cortical surface of the rat brain. Seizures induced by the neocortical and hippocampal epileptic afterdischarge models consistently displayed a slow increase in cerebral tissue impedance which reached its peak in phase with the end of the seizure and was correlated in magnitude to both ECoG/LFP recordings and fast neural impedance changes during ictal spikes that were obtained concurrently. EIT images of this slow impedance increase could be reconstructed reproducibly for both neocortical and hippocampal seizures. These revealed a focus of slow activity that was spatially confined to the facial somatosensory cortex and dentate gyrus, respectively, and progressively encompassed a larger volume over the course of the seizure. The centre of mass positions of the reconstructed slow impedance changes corresponded to the ictal foci, as determined by EEG recordings, and indicated a localisation accuracy of $\leq 200 \mu\text{m}$ for imaging as deep as the hippocampus. We therefore show that seizures possess a spatiotemporal signature due to the slow impedance response that occurs on a timescale of seconds and is a reliable marker of the underlying neural activity in the epileptogenic zone.

4.1. Technical considerations

The seizures imaged in the present study were induced by electrically stimulating the sensorimotor cortex or perforant path. This enabled controlled timing of ictal events and thus the EIT current injection protocol for imaging slow impedance changes. The employed method relied on a stable state of all seizures used for EIT recordings in a single imaging protocol. ECoG and LFP recordings confirmed that ictal foci and electrographic patterns of neocortical and hippocampal seizures were consistent over the course of experiments, as is expected in the epilepsy models utilised (Hannan *et al* 2020b), and slow impedance changes were also highly reproducible



and correlated to these electrographic features. Therefore, it was assumed that the slow impedance measurements obtained from different configurations of current-injecting electrodes during different seizures in an EIT protocol could be collated together to reconstruct a representative image of slow activity during a single ictal event. In reality, although all reconstructed impedance traces were aligned with respect to the beginning of all seizures, there was some variability in the seizure end times, and thus the time course of the slow impedance traces during the imaging protocol. This may have led to some distortion in the spatiotemporal features of reconstructed activity during the tail-end of the seizure. However, it can be argued that the ictal onset, defined as the initial discharges at the beginning of the seizure, is of highest interest for delineating epileptogenic tissue (Jehi 2018). Since the ictal onsets of seizures in a given EIT protocol were synchronised, the presented approach still provides a reliable method for localising the epileptogenic zone with high spatial accuracy using the slow impedance response. Nonetheless, the issue of variable seizure end times when using the described serial EIT method, in which impedance recordings are obtained during consecutive seizures, can be overcome in the future by use of a parallel multifrequency EIT system.

Parallel EIT systems, which are based on frequency division multiplexing, employ the simultaneous injection of current through multiple electrode pairs at different carrier frequencies (Dowrick *et al* 2015). As such, multiple impedance measurements from different current-injecting electrode pairs can be obtained in parallel during a single ictal event, thus avoiding the need for obtaining recordings from many reproducible seizures. Such a system could not be used in the present study as it is currently not possible to image fast neural activity using this approach due to the limited range of carrier frequencies that provide an adequate SNR for the associated impedance changes (Faulkner *et al* 2018a, Hannan *et al* 2018b). For this reason, a serial EIT approach was utilised to enable direct comparison of the reconstructed slow activity during seizures and fast neural activity during averaged ictal discharges. Since this work has shown that slow impedance responses reconstruct to the same location as the spike-related fast neural impedance changes, it encourages continuation of the development of parallel EIT systems for single-shot imaging of epileptic events.

For the hippocampal EIT experiments, the LFP probe was not modelled when computing the forward solution. This is unlikely to have any effect on the final image because time-difference EIT data were being reconstructed so that the effects of any such modelling errors on the final image were minimal (Brown 2003, Jehl *et al* 2016). Additionally, there was a statistically significant spatially distinct volume of common active voxels which reconstructed to the expected location across all rats in these experiments ($p < 0.03125$, $N = 5$ rats). As this was not observed in baseline or post-mortem controls that were subjected to the same EIT protocols and experimental setup, this supports the view that the reconstructed impedance changes were not artefactual.

4.2. Spatiotemporal characteristics of slow impedance changes during seizures and correlation to EEG and fast neural EIT recordings

The steady rise in tissue impedance observed during neocortical and hippocampal seizures in the present study is comparable to that described previously. Previous *in vivo* studies reported local impedance changes of $\sim 3.5\%$ – 5% in cortical and subcortical brain regions during both chemically- and electrically induced seizures in rabbits and cats, when using a carrier frequency of 1 kHz (Van Harreveld and Schadé 1962, Elazar *et al* 1966). These results are in agreement with the local impedance change of $4.33\% \pm 0.89\%$ recorded during neocortical seizures in the current work. Vongerichten *et al* (2016) measured an increase in cortical tissue impedance of $\sim 2.2\%$ during seizures induced by the chemoconvulsant 4-aminopyridine in a rat seizure model, when using current injected at a frequency of 1.7 kHz. Despite the fact that the same carrier frequency was used here to obtain EIT recordings during neocortical seizures, the slow impedance increase of $\sim 2.2\%$ is smaller than the $\sim 4.3\%$ increase observed in our study (Vongerichten *et al* 2016). This difference in magnitude may be explained by the differing properties of the seizure models used in the two studies. Unlike chemoconvulsants, the neocortical epileptic afterdischarge model does not exhibit cell-type specificity as seizures are induced by electrical stimulation which is by nature an unspecific method of activating neuronal populations (Kandratavicius *et al* 2014, Hannan 2019). Therefore, it is possible that a greater number of cortical pyramidal neurons are activated to fire in synchrony during electrically induced seizures compared to chemically-induced seizures, giving rise to the larger impedance increase observed here. Wang *et al* (2017) have also investigated the feasibility of EIT for monitoring seizures in real time. In contrast to the aforementioned studies, they reported an average impedance decrease of 4.86% – 9.17% from the surface of the cortex during seizures induced by injecting penicillin into the rat brain (Wang *et al* 2017). This result differs from the impedance increase that is expected during seizures based on modelling which was consistently seen in our study as well as the other previous studies that have investigated seizure-related impedance changes (Van Harreveld and Schadé 1962, Elazar *et al* 1966, Fabrizi *et al* 2006, Vongerichten *et al* 2016, Hannan *et al* 2018b, Avery *et al* 2019). However, this apparent discrepancy may be explained by the fact that Wang *et al* utilised a carrier frequency of 50 kHz, which is higher than that used in the other studies (Wang *et al* 2017). At frequencies ≥ 50 kHz, the applied current is expected to cross the highly resistive neuronal cell membrane and be conducted through the intracellular as well as extracellular fluid (Holder 2005, Seoane *et al* 2005). As a result, cell swelling is expected to have considerably less impact on the measured tissue impedance at such frequencies and, since blood is more conductive than the encephalic tissue, the reported impedance decrease can be explained by increased cerebral blood flow during seizures (Wang *et al* 2017).

Compared to previous studies that have characterised the slow impedance response during seizures, the present work has shown for the first time that EIT can be used to reliably and reproducibly image the slow impedance response during cortical and subcortical seizures in 3D on an anatomically realistic brain model with high localisation accuracy from the surface of the cortex. By using carrier frequencies at which fast neural impedance changes can be recorded concurrently to the slow activity, this work represents the first direct comparison of the slow and fast neural impedance changes during the same ictal events to assess the relationship between these signals. As our results have shown that the reconstructed slow activity is correlated both to EEG and fast neural EIT recordings, they suggest that the slow impedance response is indeed a reliable marker of neural activity during epileptic events and thus may be used for localising epileptogenic tissue *in vivo* and clinically.

The peak amplitude of the slow impedance response during hippocampal seizures measured with epicortical electrodes ($0.52\% \pm 0.06\%$) was expectedly an order of magnitude smaller than that recorded during neocortical seizures ($4.33\% \pm 0.89\%$). This reduction in magnitude of the slow impedance change, following an increase in depth of the source of activity from the cortical surface, is comparable to that observed in fast neural EIT ($-0.31\% \pm 0.06\%$ and $-0.041\% \pm 0.013\%$ for neocortical and hippocampal ictal discharges, respectively, measured with epicortical electrodes) (Hannan *et al* 2018a, 2020a) and can be attributed to the effects of volume conduction through cerebral tissue.

For both neocortical and hippocampal seizures, this work indicated the existence of a correlative relationship between the peak amplitude of the slow dZ and that of the averaged ictal spikes observed in the

ECoG or LFP recordings. Additionally, the peak amplitudes of the slow and fast neural dZ were significantly correlated and the peak slow dZ was consistently time-matched to the end of the seizure. However, the magnitude of this slow impedance increase was not significantly related to seizure duration. These findings support the view that the slow impedance response during seizures is caused by cell swelling following extensive ion translocation and water movement from the intracellular to extracellular space, as a result of a disturbance in ion homeostasis due to the high metabolic demands of excessive neuronal activity, and that the extent of cell swelling is proportional to the degree of hypersynchronous neuronal firing underlying the epileptiform event (Andrew and MacVicar 1994, Dzhala *et al* 2000, Dreier *et al* 2011). The lack of correlation between the seizure duration and the magnitude of the slow impedance response may be explained by the fact that the amount of cell swelling that occurs in the implicated neural tissue becomes saturated once the maximum capacity for cells to swell is reached, which can occur even before the end of the seizure (Ullah *et al* 2015). Therefore, the extent of cell swelling, and thus the size of the associated impedance response, may reach its maximal value as a result of the sustained high-frequency neuronal depolarisation during the seizure, regardless of the total seizure duration.

The slow impedance response was reconstructed reproducibly, with a temporal resolution of 1 s, in EIT images of neocortical and hippocampal seizures. For the former, the slow activity was localised to the S1 facial somatosensory cortex. This is consistent with the established importance of facial projections within the somatosensory cortex for the initiation and expression of spike-and-wave activity during neocortical seizures, as shown in previous studies that have employed genetic absence epilepsy models (Sitnikova and van Luijtelaaar 2004, Meeren *et al* 2005, Polack *et al* 2009). Unlike the fast neural EIT images of averaged SWDs which displayed a bimodal spatial profile of activation (Hannan *et al* 2018a), the slow impedance changes reconstructed over the course of the seizure were unimodal in nature and consisted of a single active volume which increased in size as the seizure progressed. This difference may be explained by the fact that it was inherently different patterns of activity, with differing biophysical properties, that were being imaged in the two setups. Whereas the fast neural EIT images showed significant neural activity during a single ictal SWD, constructed from averaging many individual repeatable SWDs during the seizure to obtain an adequate SNR for imaging, the slow activity displayed the metabolic changes which occur secondarily to neural activity over the course of the entire seizure. The neocortical seizures occasionally also contained other more variable ictal discharges, such as sharp waves and polyspike complexes, in addition to the repeatable SWDs that were identified and averaged for fast neural imaging. Therefore, it is possible that the significant slow activity observed at the FWHM threshold is localised to the neural tissue in which metabolic demands are particularly heightened during the seizure and thus represents the general epicentre of the several patterns of epileptiform activity that occur as the seizure evolves over time. In contrast, the fast neural reconstructions reflect the activation of specific neural circuits implicated in SWDs, the only type of ictal discharge that was seen consistently in all seizures in all animals and was thus suitable for averaging; this may explain why a second volume of activity is seen in fast neural EIT images ~4 ms after the first (Hannan *et al* 2018a). Nevertheless, the position of the centre of mass of the reconstructed slow activity corresponded to (a) the centre of mass of the most anterior of the two volumes of fast neural activity, which was the largest volume of active voxels and also occurred at an earlier time point than the second volume of activity, as well as (b) the true ictal focus of seizures, as determined by ECoG recordings. This suggests that the positions of the seizure onset zone localised using slow and fast neural EIT were in agreement and matched its true location.

For hippocampal seizures, the slow impedance response was reconstructed to the dentate gyrus. This is consistent with the mechanisms underlying granule cell population spikes, the fundamental component of seizures induced by electrically stimulating the perforant path, each of which is the electrophysiological manifestation of action potential synchronisation from a given population of dentate granule cells (Andersen *et al* 1971, Bragin *et al* 1997, Shepherd 2004). The localisation accuracy of the reconstructed slow activity, determined by comparing its centre of mass to the true ictal focus as determined by LFP recordings from the dentate granule cell layer, was $\leq 200 \mu\text{m}$. This contrasted to a localisation accuracy of $\leq 400 \mu\text{m}$ obtained in fast neural EIT images of averaged ictal granule cell population spikes (Hannan *et al* 2020a). The slow impedance response, therefore, offers a superior localisation accuracy for imaging epileptiform activity in deeper brain regions from the cortical surface.

4.3. Depth sensitivity of EIT for imaging slow impedance changes

The depth sensitivity of fast neural EIT for imaging ictal events from the surface of the cerebral cortex has been shown to extend to the hippocampus in the rat (~3 mm), corresponding to $>1/3$ of the total brain depth (Hannan *et al* 2020a). The present study suggested that, at this same depth, hippocampal ictal events can be localised with improved accuracy ($\leq 400 \mu\text{m}$ to $\leq 200 \mu\text{m}$) if the slow impedance response is imaged instead. This can be attributed to the greater magnitude of slow impedance changes, which are approximately ten times larger than their fast neural counterparts. Although a comprehensive analysis of the depth resolution of EIT for

imaging epileptiform activity was outside the scope of this study, our results suggest that imaging the slow impedance signal in deeper brain structures (>3 mm from the cortical surface) is promising. While fast neural activity in the thalamus during somatosensory evoked potentials cannot be imaged with EIT (Faulkner *et al* 2018b), the greater magnitude of the slow impedance response may render it possible to image thalamic epileptiform activity using non-penetrating epicortical electrodes. If the proposed EIT approach was translated to the clinical setting and a comparable arrangement of epicortical electrodes was implemented, the depth sensitivity of this method would scale up to enable imaging of the slow impedance response in at least the outer third of the human brain (Faulkner *et al* 2018b, Hannan *et al* 2020a). The volume of epileptogenic tissue implicated in seizure generation is expected to be larger in humans than in rats due to the comparatively larger anatomy of the human brain (Witkowska-Wrobel *et al* 2018, Hannan 2019). Additionally, subdural grids that are used clinically in the presurgical evaluation of epilepsy patients can contain as many as 64 electrodes, each with a typical diameter of 2–4 mm (Wyler 1992, Diehl and Lüders 2000, Voorhies and Cohen-Gadol 2013). Therefore, the proportionally larger intracranial electrodes, greater electrode coverage and larger volume of epileptogenic tissue in humans would all contribute to a depth sensitivity and localisation accuracy for imaging the slow impedance response that are proportionally comparable to that seen in the *in vivo* rat brain setup, that is at least a third of the depth of the brain and of the order of millimetres, respectively (Witkowska-Wrobel *et al* 2018, Faulkner *et al* 2018b). This can be further enhanced by using an optimised EIT protocol if any *a priori* information is available regarding the expected location of neural activity or if intracranial depth electrodes are also implemented (Witkowska-Wrobel *et al* 2018).

In the present study, EIT measurements were obtained with epicortical electrodes because we aimed to directly compare the reconstructed slow impedance response during seizures to images of the fast neural impedance response during ictal spikes, and the latter cannot currently be detected from the surface of the scalp due to its low SNR (Vongerichten *et al* 2016, Hannan *et al* 2018a, 2020a). Therefore, assessing the feasibility of imaging slow seizure-related activity with EIT using scalp electrodes was beyond the scope of this work. However, in light of our findings, which have shown that the slow impedance response is indeed a reliable marker of neural activity in the epileptogenic zone, we are currently undertaking *in vivo* experiments to assess the technical accuracy with which EIT can be used to image the slow impedance change non-invasively from the scalp in a rat seizure model. The seizure-induced slow impedance signal is expected to have a magnitude of the order of 0.1% on the scalp (Fabrizi *et al* 2006). Based on recent in-house modelling and tank experiments, we expect to be able to image signals of this magnitude non-invasively with EIT using scalp electrodes both in the rat and human brain (Avery *et al* 2019). Using a parallel multifrequency EIT system will help to improve the compatibility of our setup with the standard EEG monitoring methods used clinically and will ensure that sufficient slow impedance data can be collected in epilepsy patients who are undergoing EEG monitoring with scalp electrodes (Dowrick *et al* 2015, Avery *et al* 2019). The ability to image seizure-related slow impedance responses non-invasively with scalp electrodes would also improve the practicality of EIT for investigating the mechanisms of epileptogenesis *in vivo* to ultimately aid the development of novel anticonvulsant therapies.

4.4. Implications of the slow impedance response for clinical and *in vivo* applications

Since this work has shown that EIT images of the slow impedance response to epileptiform events in the neocortex and hippocampus are indeed representative of the underlying neural activity in the epileptogenic zone, it supports the development and use of a parallel EIT system employing simultaneous current injection at multiple frequencies for single-shot imaging of seizures. This is attractive from a clinical perspective as seizures occur unpredictably and often infrequently and so the ability to reconstruct slow changes from individual seizures would considerably reduce the total recording time. Additionally, use of a parallel EIT system would avoid the need for switching of current-injecting electrodes and thus eliminate the possibility of contaminating the clinical EEG recordings with low-frequency switching artefacts (Dowrick *et al* 2015). As such, this method could be used in conjunction with conventionally used EEG monitoring techniques to provide additional diagnostic data, obtained using standard pre-implanted intracranial EEG electrodes, during the presurgical evaluation of refractory epilepsy patients undergoing surgery without disrupting the current clinical practice. Compared to EEG, EIT has a unique solution to the inverse problem (Somersalo *et al* 1992). This contrasts with EEG inverse source localisation methods in which it may be possible for multiple current models to fit the recorded data (Jatoi *et al* 2014). In addition, because transfer impedances are measured for every current-injecting electrode pair in an EIT protocol, a greater number of independent measurements can be obtained using the same number of electrodes with EIT compared to EEG ($O(n^2)$ for EIT versus $O(n)$ for EEG, when using n electrodes) (Aristovich *et al* 2018). As such, utilising EIT increases the overall spatial and temporal information that is used to reconstruct images and localise epileptic activity. Finally, EEG source reconstruction methods are, unlike EIT, sensitive to the orientation of the source. This may lead to signal cancellation in the EEG if the epileptic activity originates from sources that are oriented tangentially to the scalp or extend over sulci or gyri

with opposing source orientations (Lüders 2008, Ahlfors *et al* 2010, Schomer and Lopes da Silva 2010). For these reasons, utilising EIT alongside standard EEG monitoring methods would enable more accurate localisation of the epileptogenic zone, the target of resection, and ultimately improve surgical outcome in these patients (Witkowska-Wrobel *et al* 2018).

If translated to clinical settings for aiding presurgical localisation of the epileptogenic zone in epilepsy patients, the lowest carrier frequency at which current should be applied is 1.355 kHz, which was used for the hippocampal imaging experiments in the present study and would ensure that EEG recordings during the standard presurgical monitoring of patients are not contaminated (Avery *et al* 2019). The magnitude and SNR of the slow impedance response during seizures is not significantly different across frequencies in the 1–10 kHz range, and so frequencies between 1.355 and 10 kHz could be used initially with parallel EIT systems (Hannan *et al* 2018b). However, it may be possible to use higher frequencies up to 50 kHz. It would be valuable, therefore, to determine the frequency response of the slow impedance change at higher frequencies prior to clinical use. The number of carrier frequencies that can be used at once is restricted by hardware limitations, which will dictate the number of current sources that can operate in parallel, as well as the number of implanted intracranial electrodes that are available for current injection which will vary across patients according to the type and extent of epileptic activity. The recommended current level to use in clinical settings is 50 μ A, the lower of the two current levels used in the present work. Since the slow impedance change during seizures is approximately ten times larger than the fast neural response during ictal discharges, we expect to be able to image seizure-related slow activity in both cortical and subcortical brain regions from the surface of cortex at this current amplitude (Hannan *et al* 2018b). Even at 1.355 kHz, the lowest frequency suggested for clinical use, current applied at 50 μ A is well below the maximum level allowed under the guidelines specified in the International Electrotechnical Commission (IEC) 60601-1 medical safety regulations and is therefore considered safe for clinical use (IEC 60601-1 2005).

Imaging the slow impedance response could also be beneficial to *in vivo* studies investigating the mechanisms of epileptogenesis. Although fast neural EIT can directly image neural activity over milliseconds, it requires averaging over repeated neural events and the magnitude of the signal is relatively small at $\sim 0.4\%$ locally (Hannan *et al* 2018a). EIT of the slow impedance response has a lower temporal resolution of seconds. However, the signal is around ten times larger and so it offers a complementary approach to image epileptic activity which is possible without the need for averaging and with an improved depth sensitivity. Therefore, the present findings complement the previously published fast neural EIT approach. There are still certain applications in which imaging the fast neural impedance response directly is preferable, for example, to elucidate neural network dynamics during epileptic discharges (Vongerichten *et al* 2016, Hannan *et al* 2018a, 2020a). Here, we have described an approach to improve the overall practicality of EIT which offers a valuable additional method that may be more feasible for certain applications, such as imaging seizures that occur spontaneously. Moreover, imaging the fast neural and slow impedance response simultaneously with EIT would increase the physiological information that is obtained during seizures and thus may provide a method for studying the mechanisms of neurovascular coupling in epileptogenesis, a phenomenon that is at present poorly understood. Overall, the choice of whether the fast neural or slow impedance response, or both, should be imaged with EIT is application-specific and should be determined by considering the specific clinical or research questions under investigation.

While it was beyond the scope of the present work, it would be of interest in the future to definitively determine whether the impedance increase is indeed caused by cell swelling and thereby investigate the relative contribution of other factors such as increased cerebral blood flow and temperature, if any, on this response. This may be explored by recording the impedance changes using carrier frequencies above 50 kHz, at which the applied current is expected to cross the neuronal cell membrane and be conducted through the intracellular as well as extracellular fluid (Holder 2005, Seoane *et al* 2005). A decrease in the magnitude of the slow impedance response at such frequencies would confirm that the impedance change observed during seizures is caused by cell swelling and could further provide insights into the mechanisms of ictogenesis and neurovascular coupling in epilepsy.

4.5. Conclusion

This work has shown that EIT can be used to image the slow impedance response during seizures that have neocortical and hippocampal foci with high reproducibility and localisation accuracy from the surface of the rat cortex. Additionally, our findings reveal that this slow increase in impedance presents a reliable surrogate marker of ongoing neural activity for localising the ictal focus. As such, EIT may be utilised, as an adjunct imaging modality to conventional EEG methods, for improving localisation of the epileptogenic zone in individuals with refractory epilepsy undergoing surgical treatment for seizure control. Future work should focus on continuing the development of a parallel multifrequency EIT system that would allow for images of the slow impedance change to be reconstructed from multiple transfer impedance measurements obtained during an

individual seizure and subsequently proceed with clinical testing. In addition to its proposed benefits for clinical settings, this system would increase the applicability of EIT as a standard *in vivo* neuroimaging tool for investigations into the pathophysiology of refractory epilepsies to ultimately direct the design and development of novel therapeutic strategies for these disorders.

Acknowledgments

This work was supported by grants from DARPA (N66001-16-2-4066), Blackrock Microsystems and the EPSRC (EP/M506448/1). James Avery was supported by the NIHR Imperial BRC.

ORCID iDs

Sana Hannan  <https://orcid.org/0000-0003-2241-8312>
Kirill Aristovich  <https://orcid.org/0000-0002-2924-5680>
Mayo Faulkner  <https://orcid.org/0000-0001-5427-0282>
James Avery  <https://orcid.org/0000-0002-4015-1802>
David S Holder  <https://orcid.org/0000-0003-2755-6124>

References

- Ahlfors S P, Han J, Lin F, Witzel T, Belliveau J W, Hämäläinen M S and Halgren E 2010 Cancellation of EEG and MEG signals generated by extended and distributed sources *Hum. Brain Mapp.* **31** 140–49
- Andersen P, Bliss T V and Skrede K K 1971 Unit analysis of hippocampal population spikes *Exp. Brain Res.* **13** 208–21
- Andrew R D and MacVicar B A 1994 Imaging cell volume changes and neuronal excitation in the hippocampal slice *Neuroscience* **62** 371–83
- Aristovich K, Donegá M, Blochet C, Avery J, Hannan S, Chew D J and Holder D S 2018 Imaging fast neural traffic at fascicular level with electrical impedance tomography: proof of principle in rat sciatic nerve *J. Neural Eng.* **15** 056025
- Aristovich K Y, Packham B C, Koo H, dos Santos G S, McEvoy A and Holder D S 2016 Imaging fast electrical activity in the brain with electrical impedance tomography *Neuroimage* **124** 204–13
- Aristovich K Y, Sato dos Santos G, Packham B C and Holder D S 2014 A method for reconstructing tomographic images of evoked neural activity with electrical impedance tomography using intracranial planar arrays *Physiol. Meas.* **35** 1095–109
- Avery J, Dowrick T, Witkowska-Wrobel A, Faulkner M, Aristovich K and Holder D 2019 Simultaneous EIT and EEG using frequency division multiplexing *Physiol. Meas.* **40** 034007
- Bahar S, Suh M, Zhao M and Schwartz T H 2006 Intrinsic optical signal imaging of neocortical seizures: the ‘epileptic dip’ *Neuroreport* **17** 499–503
- Balestrino M 1995 Pathophysiology of anoxic depolarization: new findings and a working hypothesis *J. Neurosci. Methods* **59** 99–103
- Baumann S B, Wozny D R, Kelly S K and Meno F M 1997 The electrical conductivity of human cerebrospinal fluid at body temperature *IEEE Trans. Biomed. Eng.* **44** 220–3
- Bragin A, Penttonen M and Buzsáki G 1997 Termination of epileptic afterdischarge in the hippocampus *J. Neurosci.* **17** 2567–79
- Brown B H 2003 Electrical impedance tomography (EIT): a review *J. Med. Eng. Technol.* **27** 97–108
- de Tisi J, Bell G S, Peacock J L, McEvoy A W, Harkness W F, Sander J W and Duncan J S 2011 The long-term outcome of adult epilepsy surgery, patterns of seizure remission, and relapse: a cohort study *Lancet* **378** 1388–95
- Diehl B and Lüders H O 2000 Temporal lobe epilepsy: when are invasive recordings needed? *Epilepsia* **41** S61–74
- Dowrick T, Sato dos Santos G, Vongerichten A and Holder D 2015 Parallel, multi frequency EIT measurement, suitable for recording impedance *J. Electr. Biomp.* **6** 37–43
- Dreier J P et al 2011 Spreading convulsions, spreading depolarization and epileptogenesis in human cerebral cortex *Brain* **135** 259–75
- Dzhala V, Ben-Ari Y and Khazipov R 2000 Seizures accelerate anoxia-induced neuronal death in the neonatal rat hippocampus *Ann. Neurol.* **48** 632–40
- Elazar Z, Kado R T and Adey W R 1966 Impedance changes during epileptic seizures *Epilepsia* **7** 291–307
- Fabrizi L et al 2006 Factors limiting the application of electrical impedance tomography for identification of regional conductivity changes using scalp electrodes during epileptic seizures in humans *Physiol. Meas.* **27** S163–74
- Faulkner M, Hannan S, Aristovich J, Avery J and Holder D 2018a Characterising the frequency response of impedance changes during evoked physiological activity in the rat brain *Physiol. Meas.* **39** 034003
- Faulkner M, Hannan S, Aristovich K, Avery J and Holder D 2018b Feasibility of imaging evoked activity throughout the rat brain using electrical impedance tomography *NeuroImage* **178** 1–10
- Hannan S 2019 Imaging fast neural activity in the brain during epilepsy with electrical impedance tomography *PhD Thesis* University College London
- Hannan S, Faulkner M, Aristovich K, Avery J, Walker M C and Holder D 2018a Imaging fast electrical activity in the brain during ictal epileptiform discharges with electrical impedance tomography *Neuroimage Clin.* **20** 674–84
- Hannan S, Faulkner M, Aristovich K, Avery J and Holder D 2018b Frequency-dependent characterisation of impedance changes during epileptiform activity in a rat model of epilepsy *Physiol. Meas.* **39** 085003
- Hannan S, Faulkner M, Aristovich K, Avery J and Holder D 2019 Investigating the safety of fast neural electrical impedance tomography in the rat brain *Physiol. Meas.* **40** 034003
- Hannan S, Faulkner M, Aristovich K, Avery J, Walker M C and Holder D S 2020a *In vivo* imaging of deep neural activity from the cortical surface during hippocampal epileptiform events in the rat brain using electrical impedance tomography *Neuroimage* **209** 116525
- Hannan S, Faulkner M, Aristovich K, Avery J, Walker M C and Holder D S 2020b Optimised induction of on-demand focal hippocampal and neocortical seizures by electrical stimulation *J. Neurosci. Methods* **346** 108911
- Hansen A J 1985 Effect of anoxia on ion distribution in the brain *Physiol. Rev.* **65** 101–48

- Hille B 2001 *Ion Channels of Excitable Membranes* 3rd edn (Sunderland, MA: Sinauer Associates)
- Holder D S 2005 *Electrical Impedance Tomography: Methods, History and Application* (Bristol: Institute of Physics Publishing)
- Horesh L 2006 Some novel approaches in modelling and image reconstruction for multi frequency electrical impedance tomography of the human brain *PhD Thesis* University College London
- IEC 60601-1 2005 *Medical Electrical Equipment—Part 1: General Requirements for Basic Safety and Essential Performance* 3rd edn (Geneva: International Electrotechnical Commission)
- Jatoi M A, Kamel N, Malik A S, Faye I and Begum T 2014 A survey of methods used for source localization using EEG signals *Biomed. Signal Process. Control* **11** 42–52
- Jehi L 2018 The epileptogenic zone: concept and definition *Epilepsy Curr.* **18** 12–6
- Jehl M, Dedner A, Betcke T, Aristovich K, Klöforn R and Holder D 2015 A fast parallel solver for the forward problem in electrical impedance tomography *IEEE Trans. Biomed. Eng.* **62** 126–37
- Jehl M, Aristovich K, Faulkner M and Holder D 2016 Are patient specific meshes required for EIT head imaging? *Physiol. Meas.* **37** 879–92
- Kandratavicius L, Balista P A, Lopes-Aguiar C, Ruggiero R N, Umeoka E H, Garcia-Cairasco N and Leite J P 2014 Animal models of epilepsy: use and limitations *Neuropsychiatr. Dis. Treat.* **10** 1693–705
- Klvington K A and Galambos R 1967 Resistance shifts accompanying the evoked cortical response in the cat *Science* **157** 211–3
- Latikka J, Kuurne T and Eskola H 2001 Conductivity of living intracranial tissues *Phys. Med. Biol.* **46** 1611–6
- Lüders H 2008 *Textbook of Epilepsy Surgery* (London: Informa Healthcare)
- Meeren H, van Luijtelaaar G, Lopes da Silva F and Coenen A 2005 Evolving concepts on the pathophysiology of absence seizures: the cortical focus theory *Arch. Neurol.* **62** 371–6
- Nair D R 2016 Management of drug-resistant epilepsy *Continuum* **22** 157–72
- Oh T, Gilad O, Ghosh A, Schuettler M and Holder D S 2011 A novel method for recording neuronal depolarization with recording at 125–825 Hz: implications for imaging fast neural activity in the brain with electrical impedance tomography *Med. Biol. Eng. Comput.* **49** 593–604
- Olsson T et al 2006 Cell swelling, seizures and spreading depression: an impedance study *Neuroscience* **140** 505–15
- Paxinos G and Watson C 2013 *The Rat Brain in Stereotaxic Coordinates* 7th edn (San Diego, CA: Academic)
- Polack P O, Mahon S, Chavez M and Charpier S 2009 Inactivation of the somatosensory cortex prevents paroxysmal oscillations in cortical and related thalamic neurons in a genetic model of absence epilepsy *Cereb. Cortex* **19** 2078–91
- Ranck J B 1963 Specific impedance of rabbit cerebral cortex *Exp. Neurol.* **7** 144–52
- Rao A 2000 Electrical impedance tomography of brain activity: studies into its accuracy and physiological mechanisms *PhD Thesis* University College London
- Schomer D L and Lopes da Silva F H 2010 *Niedermeyer's Electroencephalography: basic Principles, Clinical Applications, and Related Fields* 6th edn (Philadelphia; London: Lippincott Williams & Wilkins)
- Schwartz T H 2007 Neurovascular coupling and epilepsy: hemodynamic markers for localizing and predicting seizure onset *Epilepsy Curr.* **7** 91–4
- Seoane F, Lindecrantz K, Olsson T, Kjellmer I, Flisberg A and Bågenholm R 2005 Spectroscopy study of the dynamics of the transependymal electrical impedance in the perinatal brain during hypoxia *Physiol. Meas.* **26** 849–63
- Shariff S, Suh M, Zhao M, Ma H and Schwartz T H 2006 Recent developments in oximetry and perfusion-based mapping techniques and their role in the surgical treatment of neocortical epilepsy *Epilepsy Behav.* **8** 363–75
- Shepherd G M 2004 *The Synaptic Organisation of the Brain* 5th edn (New York: Oxford University Press)
- Sitnikova E and van Luijtelaaar G 2004 Cortical control of generalized absence seizures: effect of lidocaine applied to the somatosensory cortex in WAG/Rij rats *Brain Res.* **1012** 127–37
- Somersalo E, Cheney M and Isaacson D 1992 Existence and uniqueness for electrode models for electric current computed tomography *SIAM J. Appl. Math.* **52** 1023–40
- Spencer S S et al 2005 Predicting long-term seizure outcome after resective epilepsy surgery: the multicenter study *Neurology* **65** 912–8
- Tikhonov A N, Goncharky A, Stepanov V and Yagola A 1995 *Numerical Methods for the Solution of Ill-Posed Problems* (Dordrecht, The Netherlands: Kluwer Academic Publishers)
- Ullah G, Wei Y, Dahlem M A, Wechselberger M and Schiff S J 2015 The role of cell volume in the dynamics of seizure, spreading depression, and anoxic depolarization *PLoS Comput. Biol.* **11** e1004414
- Van Harrevelde A and Schadé J P 1962 Changes in the electrical conductivity of cerebral cortex during seizure activity *Exp. Neurol.* **5** 383–400
- Vongerichten A N, Sato Dos Santos G S, Aristovich K, Avery J, McEvoy A, Walker M and Holder D S 2016 Characterisation and imaging of cortical impedance changes during interictal and ictal activity in the anaesthetised rat *Neuroimage* **124** 813–23
- Voorhies J M and Cohen-Gadol A 2013 Techniques for placement of grid and strip electrodes for intracranial epilepsy surgery monitoring: pearls and pitfalls *Surg. Neurol. Int.* **4** 98
- Wang L, Sun Y, Xu X, Dong X and Gao F 2017 Real-time imaging of epileptic seizures in rats using electrical impedance tomography *Neuroreport* **28** 689–93
- Weiss H R 1988 Measurement of cerebral capillary perfusion with a fluorescent label *Microvas. Res.* **36** 172–80
- Witkowska-Wrobel A, Aristovich K, Faulkner M, Avery J and Holder D 2018 Feasibility of imaging epileptic seizure onset with EIT and depth electrodes *NeuroImage* **173** 311–21
- Wyler A R 1992 Subdural strip electrodes in surgery of epilepsy *Epilepsy Surgery* ed H Lüders (New York: Raven Press) pp 395–8
- Yang X-F, Chang J H and Rothman S M 2002 Intracerebral temperature alterations associated with focal seizures *Epilepsy Res.* **52** 97–105